

GNSS Instantaneous Ambiguity Resolution and Attitude Determination Exploiting the Receiver Antenna Configuration

Tarig Ballal, *Member, IEEE* and C. J. Bleakley, *Senior Member, IEEE*

Abstract—A novel instantaneous method for GNSS attitude determination utilising a new phase-difference ambiguity resolution approach is presented. A triple-antenna receiver configuration with baseline constraints is exploited for ambiguity resolution. It is shown that the ambiguity resolution and attitude determination problems can be solved using simple closed and semi-closed form solutions, without using GNSS codes. Simulation results demonstrate high success rates ($> 90\%$) in most cases, even when the number of visible satellite vehicles is small.

Index Terms—GNSS, GPS, navigation, attitude determination, phase-difference, ambiguity resolution.

I. INTRODUCTION

VEHICLE attitude determination is an important *Global Navigation Satellite System* (GNSS) application that is useful for air, sea and land navigation systems [1], [2], [3], [4]. The attitude determination problem can be defined as the estimation of the 3-D orientation of the body frame geometry of the GNSS antenna configuration relative to a fixed reference frame [5]. The coordinate system represented by the body frame is commonly denoted as the *local coordinate system*, whereas the reference coordinate system is referred to as the *global coordinate system* [6].

The simplest form of the GNSS vehicle attitude determination problem is determining the pointing direction of a single baseline [7], [8]. In this case, a pointing vector with three components is obtained. Full (or 3-D) attitude can be obtained by employing multiple non collinear antenna baselines [4], [9]. The 3-D attitude can be expressed in the form of an orthogonal 3×3 *attitude matrix*, the rows of which consist of the pointing vectors of each of the three axes of the local coordinate system [5].

In most existing GNSS attitude determination methods, both GNSS *code* and *carrier-phase* information are utilised. The main source of difficulty in GNSS

attitude determination is the fact that GNSS carrier-phase is ambiguous, that is the *integer* part of the observable carrier-phase is not known. The resolution of the carrier-phase ambiguity problem is of central importance for reliable GNSS attitude determination.

The literature provides an assortment of methods for carrier-phase ambiguity resolution in the context of vehicle attitude determination [5], [7], [8], [10], [11], [12]. In most cases, these methods handle the two problems of ambiguity resolution and attitude determination simultaneously. Commonly, the problem is formulated using the *phase-double-difference*, where the phase-differences observed between a receiver pair are further differenced over *satellite vehicles* (SVs). In general, ambiguity resolution requires carrier-phase and code observations over multiple receiver pairs for multiple SVs. Normally, multiple *epochs* are used in the ambiguity resolution process.

Recently, interest in *instantaneous* attitude determination (and hence instantaneous ambiguity resolution) has been shown in the literature. In instantaneous attitude determination, only data pertaining to a single epoch is utilised, and attitude is determined on an epoch-by-epoch basis. A number of techniques have been proposed in this context [3], [4], [9]. To utilise all of the information available in a single-epoch, these techniques follow the double-difference formulation over one or multiple receiver baselines, and in some cases, e.g. [9], multiple platforms are utilised. These techniques have been reported to perform well with a large number of SVs ($\#SV > 5$). However, performance degrades as the number of SVs decreases. Therefore, most previous methods fail when $\#SV = 3$, a case of practical interest in urban environments [1].

In this paper, attitude determination and ambiguity resolution are studied using a single-difference formulation of the problem. This is motivated by the fact that a single common clock can be used by all receivers in the case of attitude determination (contrary to the case of kinematic positioning), which allows for cancellation of the receiver clock error in the phase-differences [1]. This leads to a simplified approach for attitude determination using the proposed ambiguity resolution

Tarig Ballal and C. J. Bleakley are with the Adaptive & Complex Systems Laboratory, School of Computer Science & Informatics, University College Dublin, Belfield, Dublin 4, Ireland e-mail: {tarig.ballal, chris.bleakley}@ucd.ie.

method. As in [3], [4], [9], the focus herein is on the most challenging single-epoch, single-frequency case. The proposed approach can, however, be extended to the dual-frequency and/or multiple-epoch cases for enhanced performance, but this is beyond the scope of this paper.

The proposed ambiguity resolution and attitude determination technique is based on the phase-difference ambiguity resolution method that the authors of this paper proposed in [13] and [14]. A key feature of the proposed method is that, unlike existing GNSS ambiguity resolution methods, the proposed method relies completely on exploiting the receiver configuration to facilitate the ambiguity resolution task. In other words, the receivers are configured in a way that leads to a simplified solution for the ambiguity problem. Herein, a specific triple-receiver configuration is exploited. The proposed method provides a significant reduction in computational complexity compared to existing GNSS attitude determination methods, and works even in the case of a minimum number of SVs (three) with no difficulty.

In [13] and [14], the methods were applied in the acoustic domain. Applying the approach described in [13] and [14] directly to GNSS carrier-phase data does not give satisfactory success rates. In this paper, the methods are extended to handle the GNSS ambiguity problem and improve the success rate. First, the joint ambiguity resolution and pointing vector estimation problem is dealt with. Subsequently, full attitude determination is obtained from the orthogonal pointing vectors.

The rest of this paper is organised as follows. In Section II, a summary of the ambiguity resolution approach in [13] and [14] is given. In Section III, the application of the methods in [13] and [14] to the GNSS pointing vector estimation problem is discussed and the proposed ambiguity resolution approach is explained. Section IV explains how to exploit the methods developed in Section III for full attitude determination. Section V presents an overview of the simulation environment and simulation tests conducted. The results of these simulations are presented in Section VI. The conclusions of this paper are given in Section VII.

II. THE BASIC AMBIGUITY RESOLUTION METHOD

The phase-difference ambiguity resolution approach described in [13] and [14] uses the receiver configuration depicted in Fig. 1. The three receivers are configured in a linear fashion, with the shortest two baselines having different lengths, i.e., $d_{12} \neq d_{23}$. Assuming that all the distances are measured in units of the wavelength of the frequency of interest, the ambiguity resolution method restricts the difference between the length of the shortest two baselines, $\Delta \triangleq d_{23} - d_{12}$,

such that

$$|\Delta| \leq \frac{1}{2}. \quad (1)$$

In other words, the difference in the receiver separations is restricted to be less than or equal to a half-wavelength of the operational frequency. Eq. (1) represents a sufficient condition for phase-difference disambiguation. This condition was derived from a necessary condition that can be written for the *far-field* case in the form [14]

$$|\Delta| \leq \frac{1}{1 + |\sin(\theta)|}, \quad (2)$$

where $\theta \in [-90^\circ, 90^\circ]$ is the angle that the line-of-sight (LOS) vector makes with the plane perpendicular to the receiver baselines, as illustrated in Fig. 1. The line-of-sight vector in this case pertains to a SV of interest. Note that the condition in Eq. (2) is less redundant than that in Eq. (1). However, the latter condition is more practical since the right-hand side of the inequality is a fixed quantity leading to a fixed receiver configuration. Therefore, Eq. (1) was utilised for developing the ambiguity resolution method. Note that Eq. (1) is obtained from Eq. (2) by setting θ equal to $\pm 90^\circ$.

Based on the above baseline restriction in Eq. (1), it was proven that the true phase-difference between an antenna pair can be recovered from the ambiguous phase-difference observations using the following method [13]. Let us denote the ambiguous phase-differences observed over the shortest two baselines as $\{\varphi_{12}, \varphi_{23}\} \subset [-0.5, 0.5]$. These are related to the unambiguous phase-differences, $\{\phi_{12}, \phi_{23}\} \subset [-d_{12}, d_{12}]$, by

$$\begin{aligned} \phi_{12} &= \varphi_{12} + n_{12}, \\ \phi_{23} &= \varphi_{23} + n_{23}, \end{aligned} \quad (3)$$

where $\{n_{12}, n_{23}\} \subset \mathbb{Z}$. Note that all phase components are measured in units of wavelengths.

Using (3) with the condition in (1), three candidate values for the true (unambiguous) phase-difference, ϕ_{12} , can be obtained

$$\phi_{12}(k) = \frac{d_{12}}{\Delta} (\varphi_{23} - \varphi_{12} + k), \forall k \in \{-1, 0, 1\}. \quad (4)$$

Among the three-element set, $\phi_{12}(k)$, the true phase-difference is *uniquely identifiable*, as it is the *only one* in the set that satisfies

$$\phi_{12}(k) \in [-d_{12}, d_{12}] \quad (5)$$

To summarise, given a pair of phase-differences, $\{\varphi_{12}, \varphi_{23}\}$, the true phase-difference, ϕ'_{12} , can be recovered by evaluating (4) and selecting the value that satisfies (5) as ϕ_{12} . Since a candidate phase-difference that satisfies the criterion in (5) is the phase-

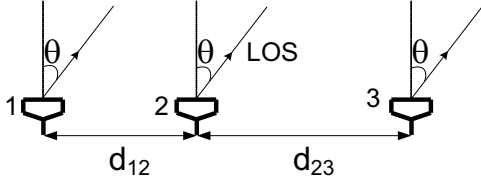


Fig. 1: Receiver antenna configuration for ambiguity resolution.

difference with the minimum absolute value, the true phase-difference can be obtained using

$$\phi'_{12} = \phi_{12}(k'), \text{ where } k' = \arg \min_k |\phi_{12}(k)|. \quad (6)$$

In the ideal case, the true phase-difference, and hence the corresponding ambiguity integer, is perfectly recovered. However, when noise is present, a non-integer value may be yielded by (3). This value can be rounded to the closest integer, i.e.,

$$\hat{n}_{12} = \lfloor \phi_{12} - \varphi_{12} \rfloor, \quad (7)$$

where $\lfloor \cdot \rfloor$ indicates the rounding operation. Next, \hat{n}_{12} is placed in (3) to obtain the final estimate of the unambiguous phase-difference as

$$\hat{\phi}_{12} = \varphi_{12} + \hat{n}_{12}. \quad (8)$$

The reader is referred to [13] and [14] for the mathematical details and proofs of Eqs. (1–8).

III. GNSS AMBIGUITY RESOLUTION AND POINTING VECTOR ESTIMATION

In this section, the method discussed in Section II is applied to the GNSS pointing vector estimation problem. The pointing vector is a unit vector or direction cosine vector that indicates the pointing direction of a line in a reference coordinate system. Pointing vector estimation is the first step towards full attitude determination. In the attitude determination context, carrier-phase information is available in the form of an ambiguous carrier-phase at each antenna. For the three-antenna configuration under consideration, the phase observations are presented in the form of three vectors; $\varphi_i \in [-0.5, 0.5]$, $i = 1, 2, 3$; each vector is of dimensions $N_{sv} \times 1$, where N_{sv} is the number of visible SVs.

The ambiguous phase-difference vectors, $\varphi_{12} \in [-0.5, 0.5]$, $\varphi_{23} \in [-0.5, 0.5]$ and $\varphi_{13} \in [-0.5, 0.5]$ are obtained using the operation

$$\begin{aligned} \varphi_{12} &= (\varphi_1 - \varphi_2) - \lfloor \varphi_1 - \varphi_2 \rfloor, \\ \varphi_{23} &= (\varphi_2 - \varphi_3) - \lfloor \varphi_2 - \varphi_3 \rfloor, \\ \varphi_{13} &= (\varphi_1 - \varphi_3) - \lfloor \varphi_1 - \varphi_3 \rfloor. \end{aligned} \quad (9)$$

The purpose of the rounding operation is to remove whole-cycle phase-difference components from the

resultant phase-differences to translate these phase-differences into the $[-0.5, 0.5]$ interval. Proper translation of phase-differences into the $[-0.5, 0.5]$ interval requires that fractional parts equal to 0.5 or -0.5 shall be set equal to zero in the rounding operation (unlike a standard rounding operation). Note that this translation is a prerequisite for the ambiguity resolution methods in [13] and [14].

A phase-difference vector, φ_{ij} , $\{i, j\} \subset \{1, 2, 3\}$, is related to the true baseline pointing vector and the satellite line-of-sight vectors by the following model:

$$\varphi_{ij} + \mathbf{n}_{ij} = d_{ij} \mathbf{R} \mathbf{a}_{true} + E, \quad (10)$$

where \mathbf{n}_{ij} and E are $N_{sv} \times 1$ vectors of the ambiguity integers and phase-difference noise, respectively; \mathbf{R} is the $N_{sv} \times 3$ matrix of the satellite line-of-sight vectors; and \mathbf{a}_{true} is the 3×1 true baseline pointing vector. Note that E is due to the phase noise contributions observed at both receiver antenna i and j . In the ideal case, when $E = 0$, $\varphi_{ij} + \mathbf{n}_{ij}$ corresponds to the true phase-difference. Given the model in Eq. (10), a pointing vector estimate can be obtained as the solution of the following minimisation problem:

$$\min_{\mathbf{a}} \|\phi_{ij} - d_{ij} \mathbf{R} \mathbf{a}\|_2^2; \quad (11)$$

subject to

$$\|\mathbf{a}\|_2 = 1; \quad (12)$$

where $\phi_{ij} = \varphi_{ij} + \mathbf{n}_{ij}$ is an estimate of the vector of the unwrapped phase-differences, and $\|\cdot\|_2$ denotes the second-order norm. The minimisation in (11) with the constrained given in Eq. (12) can be solved using the *Lagrange multiplier* method. Based on [15], the Lagrange multiplier, λ , and the pointing vector can be obtained by solving

$$(\mathbf{R}^T \mathbf{R} + \lambda \mathbf{I}) \mathbf{a} = \frac{1}{d_{12}} \mathbf{R}^T \phi_{12} \quad (13)$$

simultaneously with Eq. (12); where \mathbf{I} is a 3×3 identity matrix and $[\cdot]^T$ is the matrix transpose operation. To obtain the solution for \mathbf{a} , \mathbf{a} from Eq. (13) is substituted into Eq. (12). This yields

$$\phi_{12}^T \mathbf{R} (\mathbf{R}^T \mathbf{R} + \lambda \mathbf{I})^{-2} \mathbf{R}^T \phi_{12} - d_{12}^2 = 0. \quad (14)$$

Eq. (14) is nonlinear in λ . As suggested in [15] a number of iterative methods can be used to solve for λ . However, Eq. (14) has multiple solutions in λ (in fact, the equation can be shown to have order equal to 6). As explained in [15], out of all possible solutions of Eq. (14), the solution that minimises the cost function in (11) is the one with the largest value. Thus, we need to find the largest solution for Eq. (14). It is found by inspection that the largest root of Eq. (14) is always the closest one to zero. In this work, the required λ value is obtained by using *Newton's method* to iteratively solve Eq. (14). The iterations starts from zero and hence the

final root obtained is the largest root of the equation. This approach was found to be robust in finding the correct value of λ . This value of λ is then substituted in Eq. (13) to obtain the estimate of the pointing vector as

$$\mathbf{a} = \frac{1}{d_{12}} (\mathbf{R}^T \mathbf{R} + \lambda \mathbf{I})^{-1} \mathbf{R}^T \phi_{12}. \quad (15)$$

Now, reverting to the ambiguous phase-differences in Eq. (9), the basic disambiguation method presented in Section II is used to obtain an estimate of the vector ϕ'_{12} that represents the unambiguous phase-differences between antenna 1 and antenna 2. Next, an initial estimate of the pointing vector is obtained as the solution of the *constrained linear least squares* optimisation problem in (11). A pointing vector estimate, \mathbf{a}_0 is obtained by the substitutions $\phi_{12} = \phi'_{12}$ and $\lambda = \lambda_0$, where λ_0 is the Lagrange multiplier obtained by solving Eq. (14) for $\phi_{12} = \phi'_{12}$.

It is noted that the resultant phase-difference vector ϕ'_{12} is more noisy than the ambiguous phase-difference vectors used to obtain it. This is due to the fact that ϕ'_{12} combines the noise of the two phase-difference vectors, φ_{12} and φ_{23} (see Eq. (4)). In addition, the translation operation in (9), in some cases, results in the subtraction of an erroneous integer value. This can happen due to cycle slips caused by the accumulation of carrier-phase noise. All of these error contributions result in poor accuracy in pointing vector estimation. From simulation tests, it is found that (15) gives only a *very rough* pointing vector estimate, as will be shown in Section VI.

To improve the accuracy of pointing vector estimation, the estimate \mathbf{a}_0 is further refined using the following two steps. First, ϕ'_{12} is used to estimate the vector of the integer parts of the phase-differences across antenna 1 and antenna 2:

$$\hat{\mathbf{n}}_{12} = \lfloor d_{12} (\mathbf{R}^T \mathbf{a}_0) - \varphi_{12} \rfloor, \quad (16)$$

and a refined phase-difference vector is obtained as

$$\phi''_{12} = \varphi_{12} + \hat{\mathbf{n}}_{12}. \quad (17)$$

A refined pointing vector estimate, \mathbf{a}_1 , can now be determined as follows. First, obtain the new Lagrange multiplier, λ_1 , by setting $\phi_{12} = \phi''_{12}$ in Eq. (14) and solving (iteratively). Next, substitute ϕ''_{12} and λ_1 for ϕ'_{12} and λ_0 in Eq. (15) to obtain \mathbf{a}_1 .

To obtain the final pointing vector estimate, the phase-differences between antenna 1 and antenna 3 are used. These are the phase-differences over the longest baseline. The vector of the integer components of these phase-differences is estimated using

$$\hat{\mathbf{n}}_{13} = \lfloor d_{13} (\mathbf{R}^T \mathbf{a}_1) - \varphi_{13} \rfloor, \quad (18)$$

and the unambiguous phase-difference is now given by

$$\hat{\phi}_{13} = \varphi_{13} + \hat{\mathbf{n}}_{13}. \quad (19)$$

The final pointing vector is obtained from

$$\hat{\mathbf{a}} = \frac{1}{d_{13}} (\mathbf{R}^T \mathbf{R} + \hat{\lambda} \mathbf{I})^{-1} \mathbf{R}^T \hat{\phi}_{13}, \quad (20)$$

where, again, $\hat{\lambda}$ is obtained by iteratively in the manner explained above. Eq. (20) yields improved accuracy for $\hat{\mathbf{a}}$ compared to \mathbf{a}_0 and \mathbf{a}_1 , as will be demonstrated in Section VI.

It should be noted that the two-stage refinement can, theoretically, be reduced to only one stage by replacing \mathbf{a}_1 with \mathbf{a}_0 in (18). By comparing Eq. (18) to Eq. (16) under this replacement assumption, it can be noticed that the pointing vector estimation error is magnified by a factor equal to d_{12} for Eq. (16), and d_{13} for Eq. (18). Since $d_{13} > d_{12}$, the probability of an erroneous integer in Eq. (18) is higher when \mathbf{a}_0 is used instead of \mathbf{a}_1 . Herein, it is assumed that the ambiguous phase-differences, φ_{12} and φ_{13} , have identical noise properties. We can conclude that by using \mathbf{a}_1 instead of \mathbf{a}_0 the probability of an erroneous integer is reduced since the quality of the estimate \mathbf{a}_1 is better than that of \mathbf{a}_0 . From simulations, we found that a single-stage of refinement does not add significant improvement to pointing vector accuracy. Therefore, herein, the proposed two-stage refinement scheme is used. Another note is that, to obtain a unique solution for the pointing vector, at least three SVs are required, which is the minimum number of SVs that is considered in this work.

A. A Simplified Approach

It is noticed that the minimisation in (11) can be archived using the *unconstrained least squares* method. In fact, the cost function in (11) is *convex* and hence has a unique minimum. The least squares solution (without constraints) has the same formula as Eq. (15) for $\lambda = 0$ [16]. The resultant pointing vector form this approach may not have a unit norm. However, the pointing vector is artificially normalised to unity. This normalisation corresponds to moving the solution to the closest point that satisfies the desired constraint. Throughout the remainder of this paper the later unconstrained least squares approach will simply be referred to as the *least squares* (LS) solution. On the other hand, the alternative approach using the Lagrange multipliers will be denoted as the *constrained least squares* (CLS) solution. The CLS solution is more computationally demanding than the LS solution since the iterative method used find the Lagrange multiplier requires evaluating the right-hand side of Eq. (14) and its first derivative at each iteration. However, the CLS solution is expected to perform better than the LS solution. In the ideal (noise-free) case, all the Lagrange multipliers will be equal to zero and the two solution will coincide. It should be noted here that for more

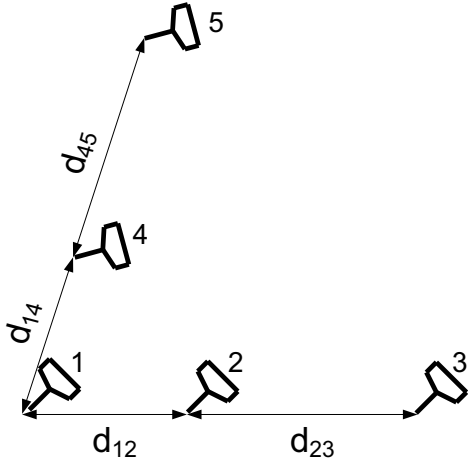


Fig. 2: Receiver antenna configuration for 3-D attitude determination.

than two SVs, the matrix $(R)^T(R)$ is nonsingular, and therefore, the inverse $(R^T R)^{-1}$ exists.

IV. THREE-DIMENSIONAL ATTITUDE DETERMINATION

To obtain 3-D attitude, we need at least a pair of non-parallel baselines. In this section, we show how to use the the proposed method for ambiguity resolution and pointing vector estimation to obtain full (3-D) attitude by employing a pair of antenna triplets. Fig. 2 shows a proposed configuration that can be utilised. In this configuration the total number of required antennas is reduced to five by having one antenna shared by two triplets. For this configuration $d_{23} - d_{12} = d_{45} - d_{14} = \Delta$. By applying the techniques from the previous section, the pointing vectors of the two (longer) baselines can be determined. Now, we have two vector observation that are known in the reference frame, as well as in the body frame. A simple algebraic method to transform such observations into attitude matrix is the TRIAD algorithm and its variants [17], [18]. Since the performance of these methods is well studied, the following sections focus on the performance of the proposed methods in estimating individual pointing vectors.

V. SIMULATIONS

To test the proposed methods, simulations were carried out. The Matlab-based GNSS VISUAL simulation software from Delft University of Technology, Netherlands, was utilised [9]. The software was not used directly, but a complete simulation was implemented using the libraries that come with the VISUAL software. The simulation was built in Matlab supporting all of the parameters that appear on the VISUAL interface.

In all simulations, a Global Positioning System (GPS) L₁ frequency (wavelength ≈ 19 cm) was used.

A cut-off elevation angle of 15° was applied. The tests were carried out over different GPS weeks. The Almanac file used in the simulation was updated to match the simulated GPS week. Time was set to 00:00, and location was set to a latitude and longitude of 50° and 3° , respectively.

Three antennas were used configured as in Fig. 1, with the difference $\Delta = d_{23} - d_{12}$ equal to 10 cm. This is slightly over the half-wavelength limit given in Eq. (1), but was found to work with the 15° cut-off elevation angle being used. This is justified from Eq. (2); by applying a cut-off elevation of 15° , $|\theta|$ is restricted to less than 15° and the necessary condition in Eq. (2) is satisfied for some baseline differences $|\Delta| > 1/2$.

In all simulations, the true carrier-phases were contaminated with Gaussian noise of zero mean and a standard deviation, σ , which was varied between 1 and 7 mm. Based on the statistical characteristics of GPS L₁ carrier-phase observations presented in [19], realistic values of σ fall between 1 and 3 mm. Therefore, it can be said that some of the test results presented herein represent challenging scenarios, namely, the tests results for values of $\sigma > 3$ mm. When the number of SVs needed for a particular test was less than the total number of visible SVs, the convention adopted was to choose the lowest-numbered SVs.

To demonstrate the performance of the proposed methods using the LS and the CLS approaches, two metrics are used. The first metric is the *success rate* (SR $\in [0, 1]$), which quantifies the ability of the proposed method to restore the correct integer vector. The second metric is the *root mean squared error* (RMSE), where the error is defined as the deviation, in degrees, of the estimated pointing vector from the true pointing vector. The two performance metrics were estimated over 10^5 trials, each trial was a simulation of the same (single) epoch. It should be noted that RMSE was only estimated over *success* cases (failure cases were excluded).

In all simulations involving the CLS approach, the initial value of λ was set equal to zero. Newton's method was used to find the solution for λ . In all cases convergence was reached after just few iterations.

VI. RESULTS

The purpose of the first set of tests was to characterise the performance of the proposed methods at different points of time. Table I lists the success rates on four different dates and GPS weeks. The baseline lengths were $d_{12} = 45$ cm and $d_{13} = 100$ cm. The standard deviation of the undifferenced carrier-phase noise was set to $\sigma = 3$ mm. The table was obtained for the $N_{sv} = 3$ case, which is the least number of SVs to yield a unique attitude solution. The entry SR₀

TABLE I: Success rates over different GPS weeks for $d_{12} = 45$ cm, $\sigma = 3$ mm and $N_{sv} = 3$.

Date	GPS week	SR ₀		SR ₁		SR	
		LS	CLS	LS	CLS	LS	CLS
02-Mar-2008	445	0.94	0.94	0.92	0.77	0.92	0.79
22-Nov-2009	535	1.00	1.00	0.97	0.98	0.93	0.93
21-May-2010	560	0.77	0.77	0.76	0.76	0.97	0.94
21-Aug-2010	573	0.98	0.98	0.96	0.96	0.96	0.96

TABLE II: Attitude RMSE over different GPS weeks for $d_{12} = 45$ cm, $\sigma = 3$ mm and $N_{sv} = 3$.

Date	GPS week	RMSE ₀ (deg.)		RMSE ₁ (deg.)		RMSE (deg.)	
		LS	CLS	LS	CLS	LS	CLS
02-Mar-2008	445	28.37	23.82	3.58	0.81	1.72	0.38
22-Nov-2009	535	9.85	8.51	1.20	0.97	0.54	0.44
21-May-2010	560	27.65	21.85	4.42	2.19	1.78	0.41
21-Aug-2010	573	8.55	6.62	1.05	0.70	0.49	0.32

is the rate at which the integer k in (4) is restored correctly for all SVs collectively, whereas SR₁ is the rate of success in recovering n_{12} using Eq. (16). On the other hand, SR is the overall success rate that coincides with the integer n_{13} (Eq. (18)). From the table, it can be seen that, in all cases, the overall success rate is reasonably high for such a challenging scenario. The relationship between SR₀ and SR₁ on one side, and the overall success rate (SR) on the other side, does not show any particular trend. However, on average, the overall success rate is higher than those of the two refinement stages. Comparing the LS with the CLS approaches; SR is very close in all cases, except for week 445, where the LS offers significantly better SR. The superiority of the CLS approach will, however, be demonstrated in the subsequent discussion when noise is increased.

Table II is the counterpart of Table I and lists the corresponding pointing vector RMSEs. These are the errors corresponding to \mathbf{a}_0 , \mathbf{a}_1 and $\hat{\mathbf{a}}$, respectively. The table shows extremely large RMSEs from the first stage for both the LS and CLS approaches. The second stage shows significant pointing vector accuracy improvement, while the final stage exhibits the finest accuracy. This demonstrates the importance of the multi-stage refinement approach. Performance differs in the four cases. This is mainly due to the satellite geometry, since all other parameters are constant. By comparing Table I and Table II, it can be concluded that there is no correlation between success rate and accuracy in the case of success. The accuracy of the CLS approach is better than that of the LS in all cases.

In the second set of tests, GPS week 573 was selected. The date was set to 21-Aug-2010. At time 00:00, 8 SVs were visible (given the 15° cut-off elevation). Two parameters were varied. The first parameter was the number of SVs involved in the computations.

The tests started by considered the first three 3 SVs (those with the lowest numbers). Subsequently, a new SV was added for each trial (the lowest consecutive number). This gives a variation of N_{sv} from 3 to 8. In addition, σ was varied from 1 to 7 mm. Fig. 3 plots success rate versus the number of SVs for different σ values. The figure shows a slight trend of increasing success rate as the number of SVs increases. This is more visible for higher σ values. For lower σ values, success rate approaches unity. The CLS approach shows noticeably higher success rate (than those of the LS approach) only with high phase noise levels. For lower phase noise value, the two approaches performs almost equivalently (in terms of success rates).

In Fig. 4, the corresponding RMSEs are plotted. Improvements in pointing vector accuracy with increases in the number of SVs can be clearly seen. The effect of carrier-phase noise is also clearly seen. Again, the CLS approach provide better performance (here in terms of pointing accuracy). This superiority is more emphasised as σ values increase. This is expected since the LS approach assumes a zero Lagrange multiplier value, an approximation whose validity reduces with high noise levels.

The results presented so far confirm the feasibility of the proposed method in resolving the phase-difference ambiguity problem. These tests have been conducted for a relatively short baseline (100-cm length). This is suitable for some applications [16]; however, other applications may require increased baseline lengths for better pointing vector accuracy. In the final test, the effect of increasing the baselines of the proposed three-antenna configuration on success rate is studied. The baseline d_{12} was varied from 45 cm (the length used in all the tests reported above) to 95 cm using a 10-centimeter increments. This resulted in the length of baseline d_{13} falling between 100 and 200 cm. Fig. 5

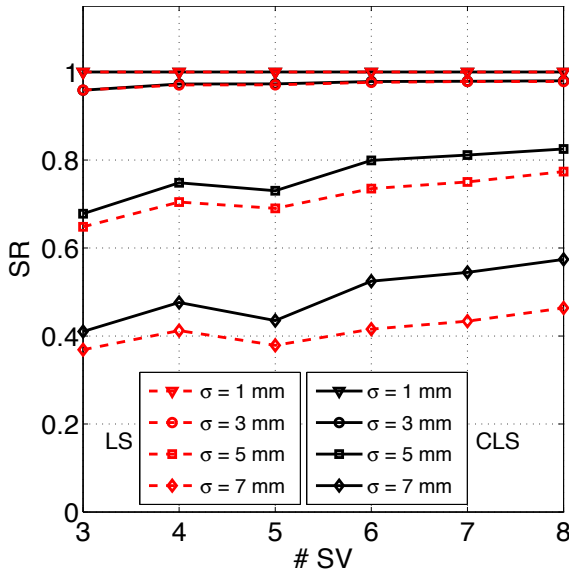


Fig. 3: Success rate (SR) versus the number of SVs (N_{sv}) for different σ values.

plots success rate against baseline length, d_{12} . The figure was plotted for the 22-Nov-2009, $\sigma = 3$ mm and $N_{sv} = 3$. Increasing the baseline length results in success rate degradation for both the CLS and LS approaches, with the latter being more susceptible to such baseline increases. For example, for baseline lengths such as $d_{12} = 95$ cm, success rate is inadequately low for the LS approach, while the CLS shows a. This effect (success rate degradation with increased baseline length) is well studied in [13] and [14]. To alleviate the problem, we suggest adding more antennas when the baseline is to be increased such that the antenna density (number of antennas per unit length) is maintained. The extended configuration should satisfy the $|\Delta| \leq 1/2$ rule for each triplet of neighbouring antennas. This approach is part of the authors' future work.

VII. CONCLUSIONS

In this paper, a method for GNSS ambiguity resolution and attitude determination was presented. The proposed method exploits a specific three-antenna configuration. Using this configuration, the ambiguity resolution and attitude determination problem was transformed in such a way that no computationally intensive optimisation step was required. Ambiguity was resolved using a simple algebraic method. The pointing vectors are estimated using either closed-form expressions or by iterative methods, resulting two different approaches. A receiver configuration and a method for full attitude determination were suggested.

The proposed method was tested in simulation. The results confirm the effectiveness of the approach in the short baseline case. It was demonstrated that, using

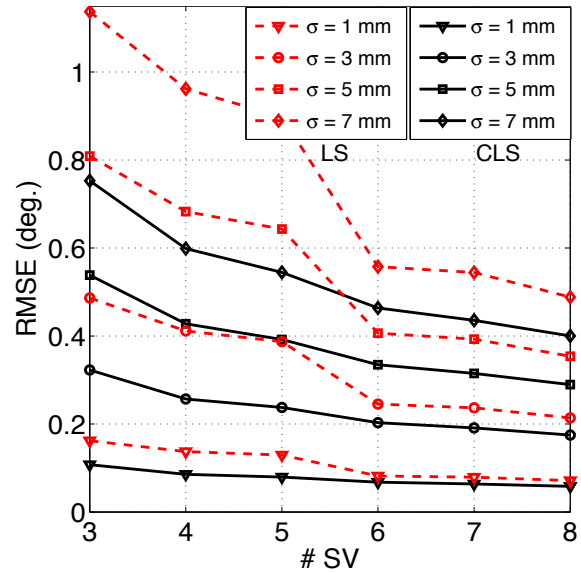


Fig. 4: The RMSE versus the number of SVs (N_{sv}) for different σ values.

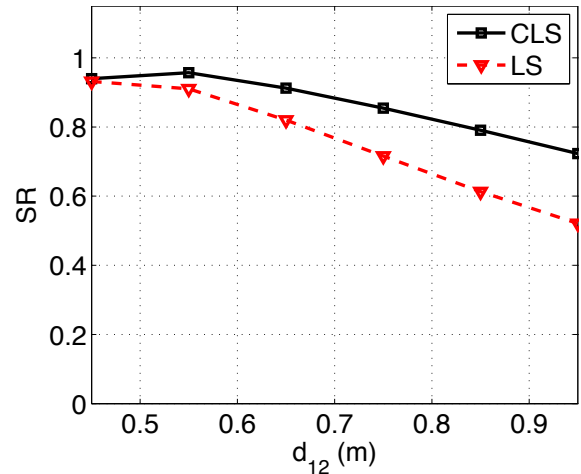


Fig. 5: Success rate (SR) versus the baseline length, d_{12} .

the proposed methods, pointing vector estimation and hence attitude determination is possible even when only as few as three satellites are visible. The two proposed approaches for pointing vector estimation perform almost equivalently with low phase noise and shorter baselines, and diverge systematically as phase noise and/or baseline lengths increase. Both methods performs acceptably with practical phase noise levels.

ACKNOWLEDGMENT

This work was funded by University College Dublin under the Seed funding programme. The authors wish to thank Gabriele Giorgi, Peter Buist and Sandra Verhagen from the Faculty of Aerospace Engineering,

Delft University of Technology, for providing the VISUAL simulation software.

REFERENCES

- [1] S. Alban, *Design and performance of a robust GPS/INS attitude system for automobile applications*, Ph.D. Dissertation, University of Stanford, 2004.
- [2] M. S. Hodgart S. Purivigraipong, M. J. Unwin and S. Kuntanapreeda, "An approach to resolve integer ambiguity of GPS carrier phase difference for spacecraft attitude determination," *IEEE Int. Region 10 Conf. TENCON 2005*, pp. 1–6, Nov 2005.
- [3] P. Buist, "The baseline constrained LAMBDA method for single epoch, single frequency attitude determination applications," *Proc. of the 20th Int. Tech. Meeting of the Satellite Division of the Institute of Navigation ION GNSS 2007*, pp. 2962–2973, Sep 2007.
- [4] P. Teunissen, G. Giorgi, and P. Buist, "Testing of a new single-frequency gnss carrier phase attitude determination method: land, ship and aircraft experiments," *GPS Solutions*, vol. 15, pp. 15–28, 2011.
- [5] C. Ferrando, A. Pérez, and R. Peña, "Integer ambiguity resolution in GPS for spinning spacecrafts," *IEEE Transactions on Aerospace and Electronic Systems*, vol. 35, no. 4, pp. 1219–1229, Oct 1999.
- [6] G. Giorgi, "The multivariate constrained LAMBDA method for single-epoch, single-frequency GNSS-based full attitude determination," *Proceedings of ION GNSS 2010*, pp. 1429–1439, Sep 2010.
- [7] R. Brown and P. Ward, "A GPS receiver with built-in precision pointing capability," *IEEE Position Location and Navigation Symposium*, pp. 83–93, Mar 1990.
- [8] C. H. Tu, K. Y. Tu, F. R. Chang, and L. S. Wang, "GPS compass: novel navigation equipment," *IEEE Trans. on Aerospace and Electronic Systems*, vol. 33, no. 3, pp. 1063–1068, Jul 1997.
- [9] P. Buist, P. Teunissen, G. Giorgi, , and S. Verhagen, "Multiplatform instantaneous gnss ambiguity resolution for triple- and quadruple-antenna configurations with constraints," *International Journal of Navigation and Observation*, vol. 2009, 2009.
- [10] G. Lu, M. Cannon, G. Lachapelle, and P. Kielland, "Attitude determination in a survey launch using multi-antenna GPS technologies," *Proceedings of National Technical Meeting, ION*, Jan 1993.
- [11] P. Teunissen, "The least-squares ambiguity decorrelation adjustment: a method for fast GPS integer ambiguity estimation," *Journal of Geodesy*, vol. 70, pp. 6582, 1995.
- [12] P. Teunissen, "The lambda method for the gnss compass," *Artificial Satellites*, vol. 41, no. 3, pp. 89–103, 2006.
- [13] T. Ballal and C. J. Bleakley, "Phase-difference ambiguity resolution for a single-frequency signal," *IEEE Signal Processing Letters*, vol. 15, pp. 853–856, Dec 2008.
- [14] T. Ballal and C. J. Bleakley, "Phase-difference ambiguity resolution for a single-frequency signal in the near-field using a receiver triplet," *IEEE Transactions on Signal Processing*, vol. 58, no. 11, pp. 5920–5926, Nov 2010.
- [15] W. Gander, "Least squares with a quadratic constraint," *Numerische Mathematik*, vol. 36, pp. 291–307, 1981.
- [16] S. Alban, "An inexpensive and robust GPS/INS attitude system for automobiles," *Proceedings of the 15th International Technical Meeting of the Satellite Division of The Institute of Navigation (ION GPS 2002)*, pp. 1075–1087, Sep 2002.
- [17] H. D. Black, "A passive system for determining the attitude of a satellite," *AIAA Journal*, vol. 2, pp. 13501351, Jul 1964.
- [18] M. D. Shuster, "The optimization of triad," *The Journal of the Astronautical Sciences*, vol. 55, pp. 245–257, 2007.
- [19] P. Cederholm, "Statistical characteristics of 11 carrier phase observations from four low-cost GPS receivers," *Nordic Journal of Surveying and Real Estate Research*, vol. 7, no. 1, pp. 58–75, 2010.